

FERROMAGNETIC MINERALS

This chapter starts with a brief introduction to magnetic properties of solids. The bulk of the chapter concerns mineralogy and magnetic properties of iron-titanium oxides and iron sulfides, which are the dominant ferromagnetic minerals. Essential aspects (such as saturation magnetization, Curie temperature, and grain-size effects) are emphasized because these characteristics strongly affect magnetic properties. A firm grasp of the mineralogy of ferromagnetic minerals is required for understanding acquisition of paleomagnetic recordings in rocks and effects of elevated temperatures and chemical changes.

MAGNETIC PROPERTIES OF SOLIDS

Figure 2.1 illustrates the three fundamental types of magnetic properties observed in an experiment in which magnetization, J , acquired in response to application of a magnetic field, H , is monitored. In this section, these different magnetic behaviors are briefly discussed. This development uses the fact that some atoms have atomic magnetic moments because of orbital and spin motions of electrons. Atomic magnetic moments are quantized, and the smallest unit is the *Bohr magneton*, $M_B = 9.27 \times 10^{-21}$ G cm³ ($= 9.27 \times 10^{-24}$ A m²). Transition element solids (principally Fe-bearing) are the common solids with atoms possessing a magnetic moment because of unfilled 3d electron orbitals. Presentation of the atomic physics leading to atomic magnetic moments can be found in Chikazumi (1964).

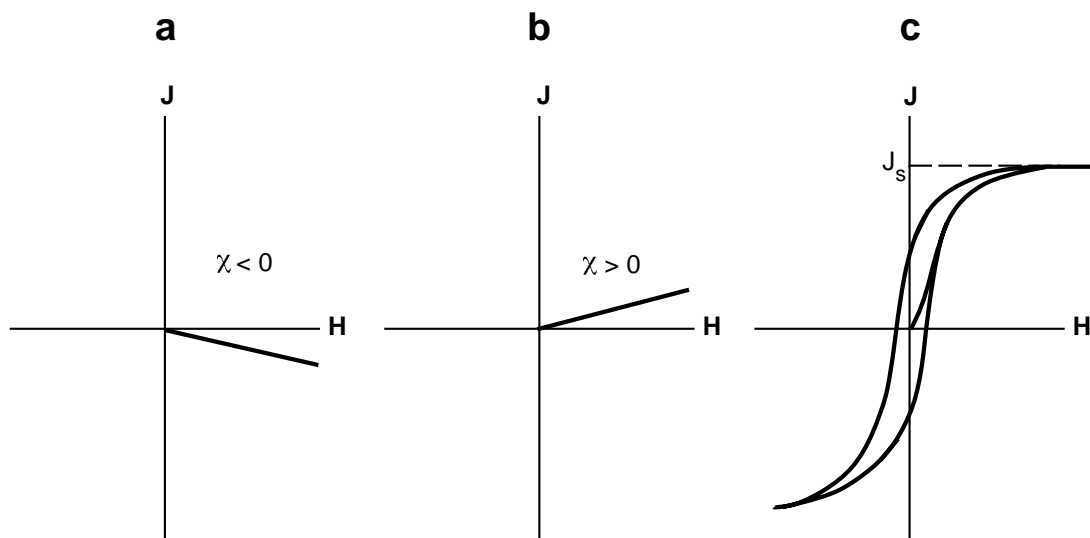


Figure 2.1 (a) Magnetization, J , versus magnetizing field, H , for a diamagnetic substance. Magnetic susceptibility, χ , is a negative constant. (b) J versus H for a paramagnetic substance. Magnetic susceptibility, χ , is a positive constant. (c) J versus H for a ferromagnetic substance. The path of magnetization exhibits hysteresis (is irreversible), and magnetic susceptibility, χ , is not a simple constant.

Diamagnetism

The *diamagnetic* response to application of a magnetic field (Figure 2.1a) is acquisition of a small induced magnetization, \mathbf{J}_i , opposite to the applied field, \mathbf{H} . The magnetization depends linearly on the applied field and reduces to zero on removal of the field. Application of the magnetic field alters the orbital motion of electrons to produce the small magnetization antiparallel to the applied magnetic field. This diamagnetic response is a property of all matter, but for substances whose atoms possess atomic magnetic moments, diamagnetism is swamped by effects of magnetic fields on the atomic magnetic moments. A material composed of atoms without atomic magnetic moments exhibits only the diamagnetic response and is classified as a diamagnetic material. Magnetic susceptibility, χ , for a diamagnetic material is negative and independent of temperature. An example of a diamagnetic mineral is quartz, SiO_2 , and a typical value of magnetic susceptibility is $\sim -10^{-6}$ in cgs units ($\sim -0.8 \times 10^{-7}$ SI).

Paramagnetism

Paramagnetic solids contain atoms with atomic magnetic moments (but no interaction between adjacent atomic moments) and acquire induced magnetization, \mathbf{J}_i , parallel to the applied field, \mathbf{H} (Figure 2.1b). For any geologically relevant conditions, J_i is linearly dependent on H . As with diamagnetic materials, magnetization reduces to zero when the magnetizing field is removed. An example of a paramagnetic mineral is fayalite, Fe_2SiO_4 , with room temperature magnetic susceptibility of $\sim 4.4 \times 10^{-4}$ cgs ($\sim 3.5 \times 10^{-5}$ SI).

In paramagnetic solids, atomic magnetic moments react independently to applied magnetic fields and to thermal energy. At any temperature above absolute zero, thermal energy vibrates the crystal lattice, causing atomic magnetic moments to oscillate rapidly and randomly in orientation. In the absence of an applied magnetic field, atomic moments are equally distributed in all directions with resultant magnetization $J_i = 0$.

Application of a magnetic field exerts an aligning torque (Equation (1.3)) on the atomic magnetic moments. The aligning energy of a magnetic moment, \mathbf{M} , in a field, \mathbf{H} , is given by Equation (1.4) as $E = -MH \cos \theta$ where θ is the angle from \mathbf{H} to \mathbf{M} . Consider an atomic magnetic moment, $M = 2M_B = 1.85 \times 10^{20}$ G cm³ ($= 1.85 \times 10^{23}$ A m²), in a magnetic field of 100 Oe ($= 10^{-2}$ T, ~ 100 times the surface geomagnetic field). The aligning energy is $MH = (1.85 \times 10^{20} \text{ G cm}^3) \times (10^2 \text{ Oe}) = 1.85 \times 10^{-18}$ erg ($= 1.85 \times 10^{27}$ J). However, thermal energy at 300°K (traditionally chosen as temperature close to room temperature, which provides easy arithmetic) is $kT = (1.38 \times 10^{-16} \text{ erg/}^\circ\text{K}) (300^\circ\text{K}) = 4.14 \times 10^{-14}$ erg, where k = Boltzmann constant. So thermal energy is 10^4 times the aligning energy; hence, magnetization is small even in this significant magnetizing field.

The *Langevin theory* provides an insightful model for paramagnetism. Consider a paramagnetic solid with N atomic moments per unit volume. The relative probability, $P(\theta)$, of an atomic moment \mathbf{M} having angle θ with the applied field \mathbf{H} is determined by statistical thermodynamics:

$$P(\theta) = \exp\left(\frac{MH \cos \theta}{kT}\right) \quad (2.1)$$

The degree of alignment depends exponentially on the ratio of aligning energy to thermal energy. Considering components of \mathbf{M} along \mathbf{H} , forcing the total number of atomic moments to equal N , and integrating over the 0 to π range of θ yield the basic result of Langevin theory:

$$J = NML(\alpha) \quad (2.2)$$

where

$$L(\alpha) = \coth(\alpha) - \frac{1}{\alpha}$$

$$\alpha = \frac{MH}{kT}$$

The function $L(\alpha)$ is the *Langevin function* plotted in Figure 2.2. Equation (2.2) predicts two intuitive results: (1) $J = 0$ for $H = 0$, because $\alpha = 0$ and $L(0) = 0$, and (2) for infinite magnetic field, $\alpha = \infty$, $L(\infty) = 1.0$, and $J = NM$, meaning that the atomic magnetic moments are completely aligned with the field.

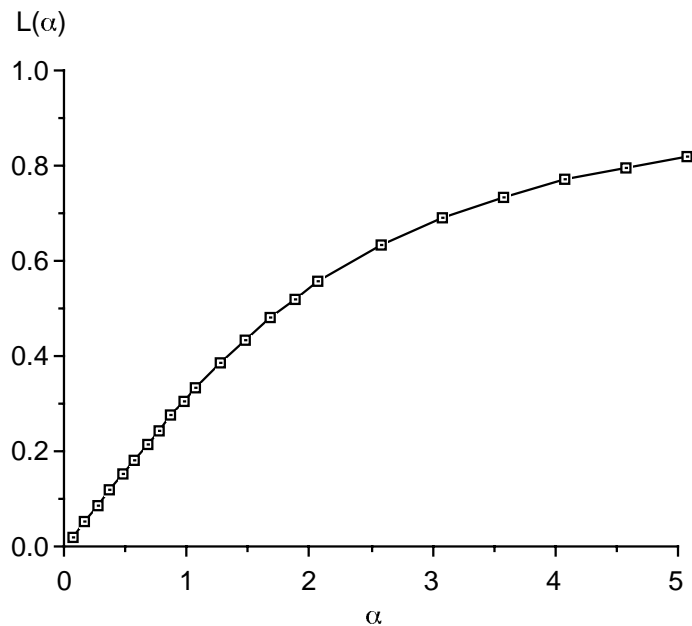


Figure 2.2 The Langevin function, $L(\alpha)$. Notice that for $\alpha < 1$, $L(\alpha) \approx \alpha/3$.

In any geologically reasonable situation, $\alpha = MH/kT$ is $< 10^{-6}$. The Langevin function is linear for $\alpha \ll 1$ with $L(\alpha) \approx \alpha/3$, and Equation (2.2) simplifies to

$$J = NML(\alpha) = \frac{NM\alpha}{3} = \frac{NM^2H}{3kT} \quad (2.3)$$

$$\chi = \frac{J}{H} = \frac{NM^2}{3kT} \quad (2.4)$$

This is the *Curie law of paramagnetic susceptibility*, which applies to any typical situation in rock magnetism. The Curie law predicts the observed constant value of paramagnetic susceptibility for a given material and temperature. In addition, the Curie law accounts for the observed $1/T$ decrease of χ with increasing temperature.

Ferromagnetism

Ferromagnetic solids have atoms with magnetic moments, but unlike the paramagnetic case, adjacent atomic moments interact strongly. The effect of interaction is to produce magnetizations in ferromagnetic solids that can be orders of magnitude larger than for paramagnetic solids in the same magnetizing field. For a given ferromagnetic material and temperature there is a maximum magnetization referred to as *saturation magnetization*, j_s (Figure 2.1c); increasing H beyond the level needed to reach j_s will not result in increased magnetization. Metallic iron is a ferromagnetic solid with saturation magnetization at room temperature $= 1.8 \times 10^3$ G (1.8×10^6 A/m).

Saturation magnetization decreases with increasing temperature, becoming zero at the *Curie temperature*, T_C , which is characteristic of the particular ferromagnetic material (580°C for magnetite and 680°C for hematite). Temperature dependences of j_s for magnetite and for hematite are shown in Figure 2.3. Above the Curie temperature, the material becomes paramagnetic.

Besides strong intensity of magnetization, the fundamental property of ferromagnetic solids that makes them the focus of our attention is their ability to record the direction of an applied magnetic field. During removal of the magnetizing field, magnetization does not return to zero but retains a record of the applied field. The path of magnetization, \mathbf{J} , as a function of applied field, \mathbf{H} , is called a *hysteresis loop*, and we will later examine hysteresis in detail. Because of hysteresis, magnetic susceptibility of ferromagnetic materials cannot be simply expressed as for diamagnetic or paramagnetic solids.

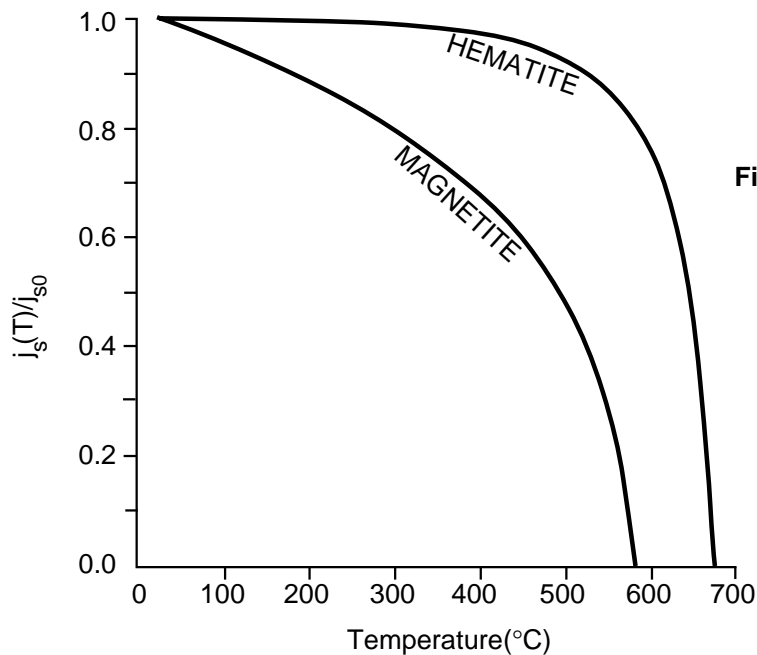


Figure 2.3 Normalized saturation magnetization versus temperature for magnetite and hematite. j_{s0} = saturation magnetization at room temperature; for hematite, $j_{s0} \approx 2$ G; for magnetite, $j_{s0} = 480$ G. Redrawn from Pullaiah et al. (*Earth Planet. Sci. Lett.*, v. 28, 133–143, 1975).

Coupling of adjacent atomic moments in a ferromagnetic material is the result of *exchange energy* of quantum mechanical nature. Classical physics does not provide an explanation for exchange energy, and rigorous understanding of exchange energy requires several years of mind-bending study. Furthermore, learning the necessary quantum mechanics has been known to disorient students. So we shall settle for a qualitative explanation of ferromagnetism.

The Pauli Principle states that only one electron per atom can have a particular set of the four quantum numbers n , l , l_z , and s_z . For an isolated atom of a transition element there is no confusion about the electron states occupied. However, for a collection of atoms within a crystal lattice, the situation can be complex. Electron orbitals are probability distributions that can have elongate shapes. Partial overlaps of electron probability distributions occur when atoms are packed together in a crystalline solid. These overlaps can develop so that electrons of adjacent atoms attempt to satisfy the Pauli Principle of both atoms simultaneously. The result is that electron states and magnetic moments of the adjacent atoms become strongly coupled. This simple view suggests how crystal structure and density of packing determine whether a solid containing transition elements is paramagnetic (no overlapping orbitals and no exchange coupling) or ferromagnetic (significant orbital overlap and resulting exchange coupling).

Because interatomic distance increases during thermal expansion, strength of exchange coupling and resultant j_s decrease with increasing temperature. At the Curie temperature, T_C , interatomic distances have increased to the point at which exchange coupling is destroyed. Atomic magnetic moments are then independent, and the material becomes paramagnetic. In general, the process is reversible, with exchange coupling and ferromagnetism again appearing when the material is cooled below T_C .

Magnetization of ferromagnetic solids to saturation is most easily achieved along certain crystallographic directions, called *magnetocrystalline easy directions*, and the crystallographic dependence of ferromagnetism is called *magnetocrystalline anisotropy*. This crystallographic directional dependence arises because electron orbitals must rotate as the atomic magnetic moments are forced to rotate. Because interatomic distances depend on crystallographic direction, the amount of orbital overlap (and resulting exchange energy) also depends on crystallographic direction. The result is magnetocrystalline anisotropy with exchange energy depending on crystallographic direction of magnetization. Magnetocrystalline anisotropy is a major source of stability for paleomagnetism in rocks and is developed more completely in Chapter 3.

Exchange energy may produce either parallel or antiparallel exchange coupling. The sense of coupling depends on the transition element involved and on crystal structure. Permutations of exchange coupling are shown in Figure 2.4. One can regard the general term *ferromagnetism* as applying to all three types of solids with coupling of atomic magnetic moments. Strictly speaking, *ferromagnetism* refers to solids with parallel coupling of adjacent atomic magnetic moments (Figure 2.4a). The situations depicted in Figure 2.4b and 2.4c involve parallel coupling within layers of atomic magnetic moments but antiparallel coupling between layers. If the layers have equal magnetic moment, opposing layers cancel, with resulting $j_s = 0$. This type of coupling is *antiferromagnetic*. If layers of unequal magnetic moment are antiparallel, the resulting j_s points in the direction of the dominant layer. Such materials are called *ferrimagnetic*, and many of the important “ferromagnetic” minerals are, in fact, ferrimagnetic. In what follows, the term “ferromagnetism” is used in the general sense to designate exchange-coupled materials. Where the exact type of coupling is important to the discussion, the terms antiferromagnetic, etc. will be used.

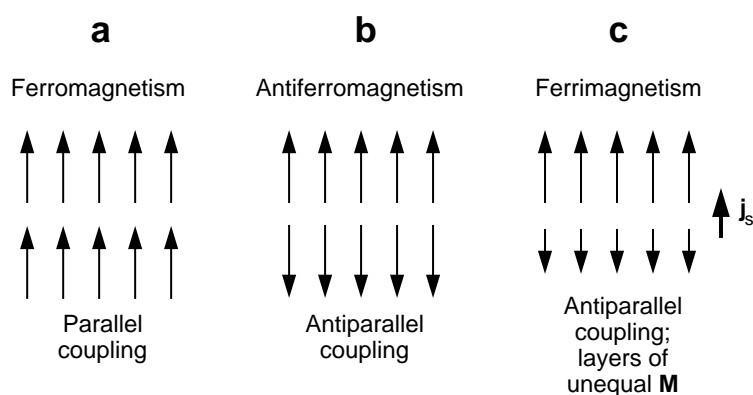


Figure 2.4 Exchange couplings for (a) ferromagnetic, (b) antiferromagnetic, and (c) ferrimagnetic materials. The net magnetization for ferrimagnetic material is shown at right; the net magnetization of antiferromagnetic material is zero.

MINERALOGY OF FERROMAGNETIC MINERALS

By far the most important ferromagnetic minerals are the *iron-titanium (FeTi) oxides*. FeTi oxides are generally opaque, and petrographic examination requires observations of polished sections in reflected light. These minerals are given little attention in standard petrology courses, which emphasize examination of thin sections in transmitted light. Accordingly, the FeTi oxides are generally an unfamiliar set of minerals. Understanding paleomagnetism requires some knowledge of the crystal chemistry and magnetic structure of FeTi oxides. This includes basic knowledge of phases formed as primary crystals from igneous melts and subsolidus reactions affecting these minerals to yield FeTi oxides encountered in igneous rocks and derivative sedimentary rocks.

Composition of the FeTi oxides are conveniently displayed on the $\text{TiO}_2\text{--FeO--Fe}_2\text{O}_3$ *ternary diagram* (Figure 2.5). Positions from left to right indicate increasing ratios of ferric (Fe^{3+}) to ferrous (Fe^{2+}) iron while positions from bottom to top indicate increasing Ti content (Ti^{4+} : total Fe). Using $(1/2)\text{Fe}_2\text{O}_3$ as the parameter for the Fe^{3+} corner normalizes the diagram to one cation, producing the convenient effect that lines of oxidation (increasing the $\text{Fe}^{3+}:\text{Fe}^{2+}$ ratio) are parallel to the base of the diagram. Two solid solution series, titanomagnetites and titanohematites, are the primary focus of our attention. Members of both series are primary crystallizing phases in igneous rocks, generally constituting from 1% to 5% by volume.

Titanomagnetites

The *titanomagnetites* are opaque, cubic minerals with compositions between end members *magnetite* (Fe_3O_4) and *ulvöspinel* (Fe_2TiO_4). The crystal structure of titanomagnetites is the *spinel structure*. A unit cell con-

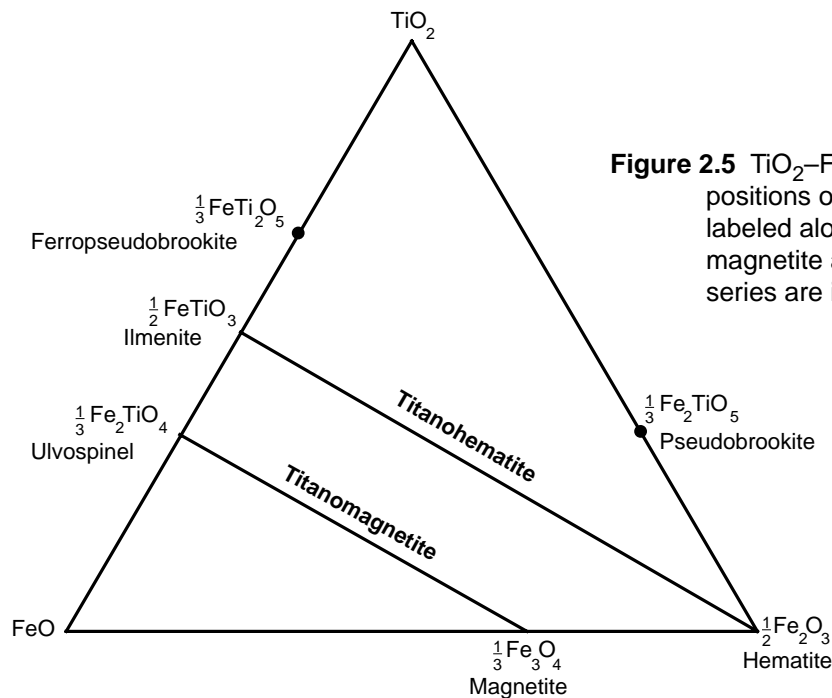


Figure 2.5 TiO_2 - FeO - Fe_2O_3 ternary diagram. Compositions of important FeTi-oxide minerals are labeled along with mineral names; titanomagnetite and titanohematite solid solution series are indicated.

tains 32 O^{2-} anions arranged in a face-centered-cubic network. These O^{2-} anions form approximately hexagonal-close-packed (111) planes orthogonal to the cube diagonal [111] direction. Within this network of O^{2-} anions, there are two types of cation sites. The *A sublattice* is made up of eight sites per unit cell in tetrahedral coordination with four surrounding O^{2-} anions. The *B sublattice* is composed of 16 sites per unit cell in octahedral coordination with six surrounding O^{2-} anions. The tetrahedral and octahedral coordinations of A and B sublattice cations are shown in Figure 2.6. Distribution of the 24 cations per unit cell within A and B sublattices and exchange coupling between these sublattices control the magnetic properties of titanomagnetites.

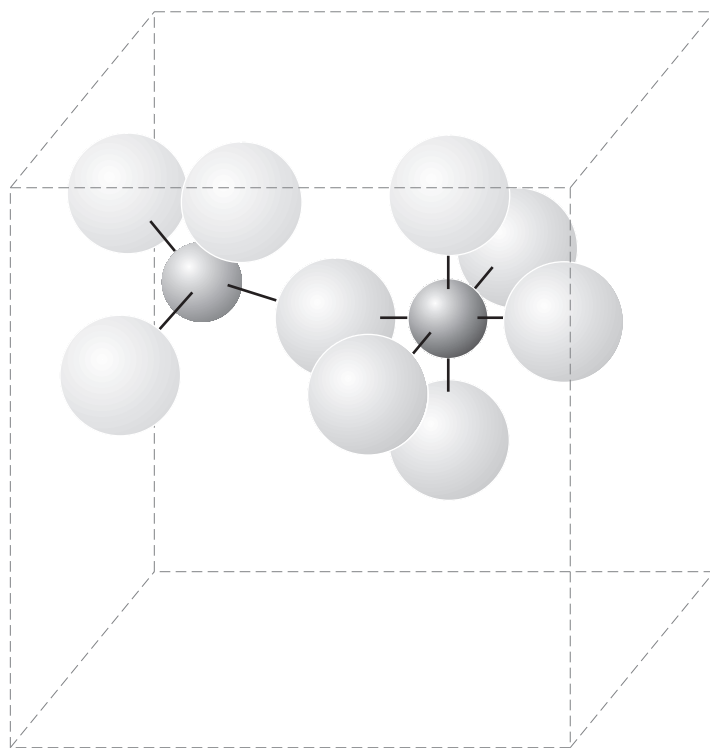


Figure 2.6 Coordinations of Fe cations with O^{2-} anions in magnetite. O^{2-} anions are lightly shaded spheres; A-sublattice cations (medium shaded spheres) are in tetrahedral coordination with four O^{2-} anions; B-sublattice cations (dark spheres) are in octahedral coordination with six O^{2-} anions; the unit cell dimension of the spinel crystal structure is shown by the dashed lines.

In magnetite, there are 16 Fe^{3+} and eight Fe^{2+} cations per unit cell. Cations distribute between the A and B sublattices in an *inverse spinel* structure. In a *normal spinel*, similar cations occupy the same sublattice. For example, ZnFe_2O_4 is a normal spinel with two Fe^{3+} cations per formula unit occupying B sites and one Zn^{2+} cation occupying the A site (Figure 2.7). In the inverse spinel structure of magnetite, the two B sites per formula unit are occupied by one Fe^{2+} and one Fe^{3+} , and the A site is occupied by the remaining Fe^{3+} .

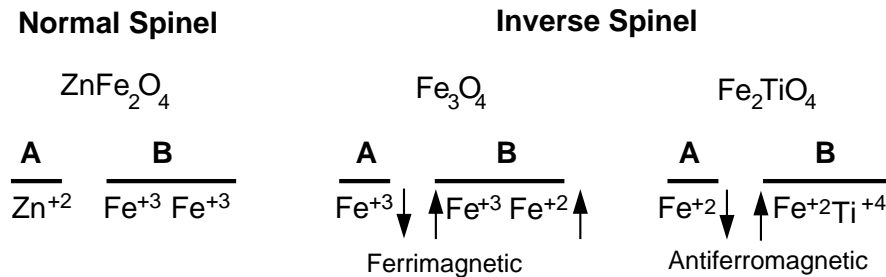


Figure 2.7 Comparison of cation distributions in normal spinel and inverse spinel. **A** and **B** indicate A sublattice and B sublattice cations, respectively; arrows indicate directions of cationic magnetic moments. Redrawn after McElhinny (*Palaeomagnetism and Plate Tectonics*, Cambridge, London, 356 pp., 1973).

Coupling of atomic magnetic moments of Fe^{2+} and Fe^{3+} cations is also shown in Figure 2.7. The exchange interaction between cations takes place through an intervening O^{2-} anion and is referred to as *super exchange* interaction. Effectively, the magnetic moments of cations within each sublattice are parallel coupled, whereas A and B sublattices are antiparallel coupled. Because the B sublattice has one Fe^{2+} and one Fe^{3+} for every Fe^{3+} cation in the A sublattice, the atomic moments of Fe^{3+} cations cancel, leaving a net magnetic moment due to Fe^{2+} cations. This antiparallel coupling of two unequal sublattices makes Fe_3O_4 ferrimagnetic. The spinel crystal structure yields a preferred direction of magnetization (= magnetocrystalline easy direction) along the cube diagonal [111]. The resulting saturation magnetization of magnetite is 480 G (4.8×10^5 A/m) (adjusted to zero thermal energy at 0°K), and the Curie temperature is 580°C.

To understand how magnetic properties vary within the titanomagnetite series, it is instructive to examine the Ti-rich end member ulvöspinel, Fe_2TiO_4 . The Ti^{4+} cations enter the inverse spinel structure in the B sublattice. Remaining Fe cations are both Fe^{2+} , as required for charge neutrality. The filled electron orbital for Ti^{4+} means that this cation does not possess an atomic magnetic moment. As illustrated in Figure 2.7, the antiparallel coupling of A and B sublattices is now between two sublattices of equal atomic moment, and ulvöspinel is antiferromagnetic. However, the Néel temperature (temperature at which antiferromagnetic coupling disappears) is -153°C , so ulvöspinel is paramagnetic at or above room temperature.

In the titanomagnetite series, Ti^{4+} substitutes for Fe^{3+} as Ti content increases. The generalized chemical formula for titanomagnetite is $\text{Fe}_{3-x}\text{Ti}_x\text{O}_4$, where x ranges from 0.0 for magnetite to 1.0 for ulvöspinel. The ionic substitution is $2\text{Fe}^{3+} \rightarrow \text{Fe}^{2+} + \text{Ti}^{4+}$, indicating that a remaining Fe cation must change valence from Fe^{3+} to Fe^{2+} for each Ti^{4+} introduced. Although it is clear that Ti^{4+} cations enter the B sublattice, the distribution of Fe^{2+} and Fe^{3+} cations between sublattices and resulting net magnetic moment for intermediate titanomagnetites is in dispute.

We use the convenient approximation (likely correct for rapidly cooled titanomagnetites) that Fe^{2+} and Fe^{3+} are equally distributed between the A and B sublattices. This yields a linear dependence of saturation magnetization, j_s , upon composition, when j_s is adjusted to 0°K. So quite sensibly, addition of Ti^{4+} (with no atomic moment) into the magnetite structure progressively decreases saturation magnetization. Equally important is the observed dependence of Curie temperature, T_C , upon Ti content. Both T_C and j_s are shown as functions of the titanomagnetite compositional parameter, x , in Figure 2.8. Any titanomagnetite with $x > 0.8$ will be paramagnetic at room temperature or above.

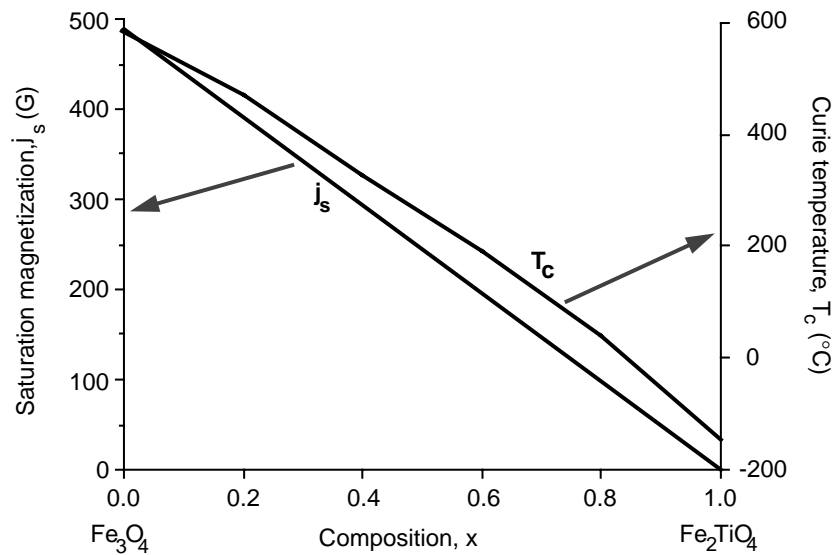


Figure 2.8 Saturation magnetization and Curie temperature for titanomagnetite series. Composition is indicated by parameter x ; the left axis indicates saturation magnetization (j_s); the right axis indicates Curie temperature (T_c). Redrawn after Nagata (1961).

Titanohematites

We wish that titanohematites were as simple as titanomagnetites, but they are not. In the presentation below, many complexities are glossed over to present essential information. (My apologies to Louis Néel, Ken Hoffman, and any other specialists in this field who might feel affronted by the simplifications employed.)

In most igneous rocks, titanohematites and their oxidation products constitute a lesser portion of ferromagnetic minerals than do titanomagnetites (and oxidation products thereof). But for highly silicic and/or highly oxidized igneous rocks, hematite can be the dominant ferromagnetic mineral. In addition, hematite is almost always the dominant or exclusive ferromagnetic mineral in red sediments, a major source of paleomagnetic data.

The titanohematites are generally opaque minerals with a magnetic structure most easily described by using the hexagonal system. Layers of approximately hexagonal-close-packed O^{2-} anions are parallel to the (0001) basal plane. For each 18 O^{2-} anions, there are 18 potential cation sites in octahedral coordination with six surrounding O^{2-} anions. In titanohematites, two thirds of these cation sites are occupied.

For hematite (denoted as $\alpha\text{Fe}_2\text{O}_3$ to avoid confusion with other forms of Fe_2O_3 introduced later), all cations are Fe^{3+} and occur in (0001) layers alternating with layers of O^{2-} anions. Atomic magnetic moments of Fe^{3+} cations lie in the basal plane orthogonal to the [0001] axis. Atomic moments are parallel coupled within (0001) planes but approximately antiparallel coupled between adjacent layers of cations. This situation is shown in Figure 2.9. However, the angle between magnetic moments of these alternate layers departs slightly from 180° , yielding a net magnetization as shown on the right side of Figure 2.9. This net magnetization lies in the basal plane nearly perpendicular to magnetic moments of the Fe^{3+} layers. Hematite ($\alpha\text{Fe}_2\text{O}_3$) is referred to as *canted antiferromagnetic* and has a saturation magnetization of ~ 2 G (2×10^3 A/m) due to this imperfect antiferromagnetism.

In addition to the magnetization from canting, some naturally occurring hematite has additional magnetization referred to as *defect ferromagnetism*, perhaps arising from (ordered structure of) lattice defects or nonmagnetic impurity cations. While the origins of the two contributions to net magnetization are complex and not fully understood, the effect is one of weak ferromagnetism with $j_s \approx 2\text{--}3$ G ($2\text{--}3 \times 10^3$ A/m). Again glossing over complications, the effective *Néel temperature* (temperature at which exchange coupling within an antiferromagnetic mineral disappears) of hematite is 680°C .

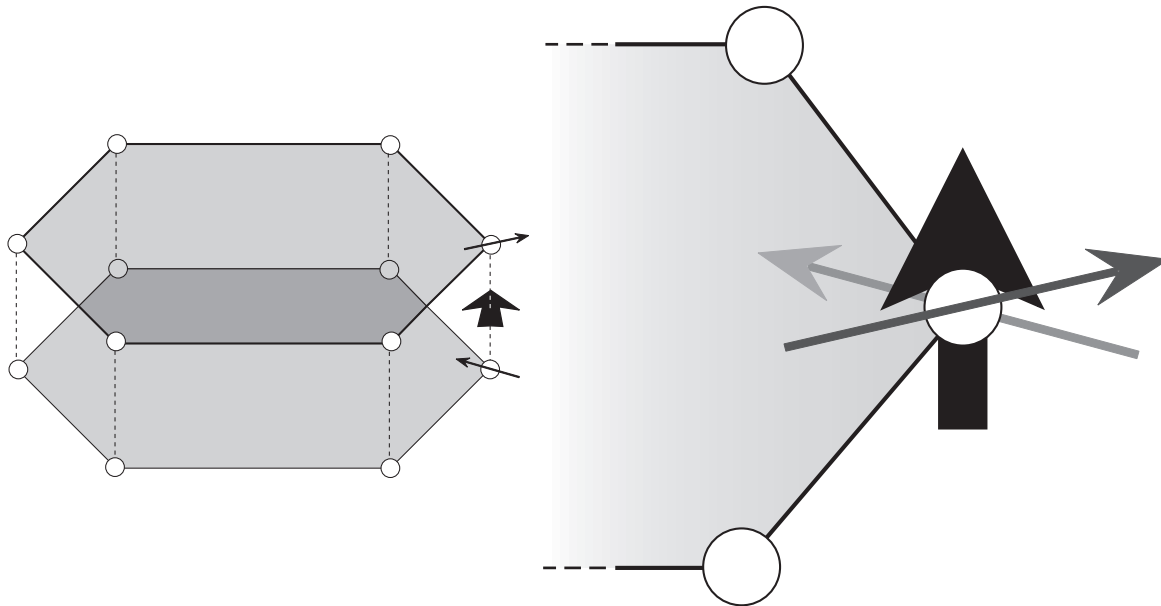


Figure 2.9 Coupling of cationic (Fe^{3+}) magnetic moments in hematite. Planes of cations are basal (0001) planes; magnetic moments are parallel within a particular basal plane; coupling of cationic (Fe^{3+}) magnetic moments between (0001) planes is shown on the right of the diagram; the magnetic moment in the upper plane is shown by the dark gray arrow; the magnetic moment in the lower plane is shown by the light gray arrow; the vector sum of these two nearly antiparallel magnetic moments is shown by the bold black arrow using a greatly expanded scale.

Turning now to *ilmenite* (FeTiO_3), Ti^{4+} layers alternate with layers of Fe^{2+} cations. Magnetic moments of Fe^{2+} cations within a particular basal plane are parallel-coupled with magnetic moment oriented along the [0001] axis. Alternating Fe^{2+} layers are antiparallel-coupled, and thus ilmenite is antiferromagnetic with Néel temperature of -218°C .

Ionic substitution in the titanohematite series is exactly as in titanomagnetites, with Ti^{4+} substituting for Fe^{3+} and one remaining Fe cation changing valence from Fe^{3+} to Fe^{2+} . The generalized formula is $\text{Fe}_{2-x}\text{Ti}_x\text{O}_3$, where x ranges from 0.0 for hematite to 1.0 for ilmenite. As shown in Figure 2.10, the “Curie” temperature has a simple linear dependence on composition. But saturation magnetization, j_s , (adjusted to 0°K) varies in a complex fashion. The explanation lies in the distribution of cations in intermediate composition titanohematites. It should be noted that titanohematites with $x > 0.8$, like titanomagnetites with high Ti content, are paramagnetic at or above room temperature.

For $0.0 < x < 0.45$, titanohematites retain the canted antiferromagnetic arrangement of hematite, with Fe and Ti cations equally distributed amongst cation layers. Over this range of compositions, saturation magnetization is approximately constant and low ($j_s \approx 2 \text{ G}$). However, for $x > 0.45$, Fe and Ti cations are no longer equally distributed; Ti cations preferentially occupy alternate cation layers. Because Ti cations have no atomic magnetic moment, antiparallel coupling of two sublattices with unequal magnetic moment develops, and titanohematites with $0.45 < x < 1.0$ are ferrimagnetic.

Intermediate titanohematites also possess an additional (mercifully) uncommon magnetic property: *self-reversal of thermoremanent magnetism*. Depending on exact composition and cooling rate, intermediate composition titanohematites can acquire remanent magnetism antiparallel to the magnetic field in which they cool below the Curie temperature. This self-reversing property is now recognized as uncommon because titanohematites of this composition are rarely the dominant ferromagnetic mineral in a rock. However, as will be discussed in Chapter 9, this self-reversing property caused confusion during early development of the geomagnetic polarity time scale.

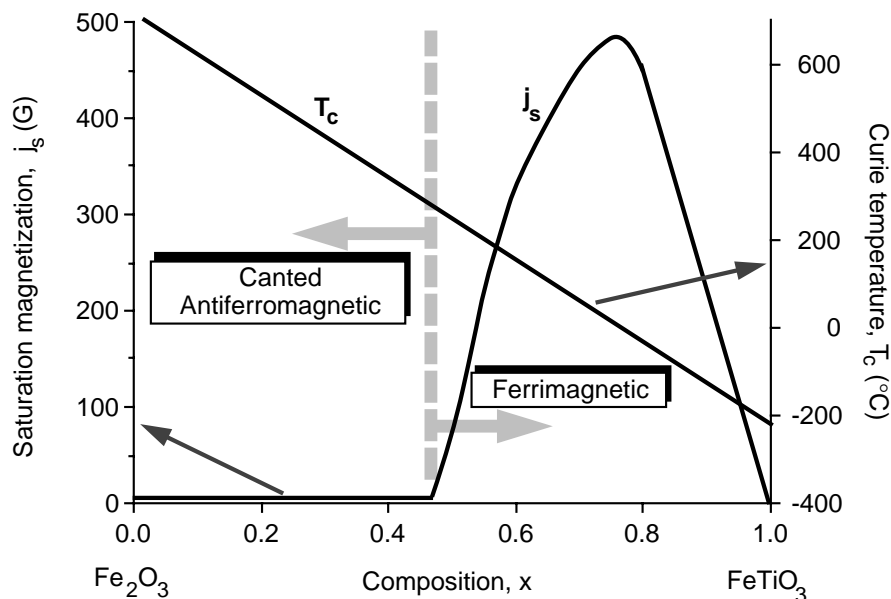


Figure 2.10 Saturation magnetization and Curie temperature for titanohematite series. Composition is indicated by parameter x ; the left axis indicates saturation magnetization (j_s); the right axis indicates Curie temperature (T_c); compositions $x < 0.45$ have canted antiferromagnetic coupling; compositions $0.45 < x < 1.0$ have ferrimagnetic coupling. Modified from Nagata (1961) and Stacey and Banerjee (1974).

Primary FeTi oxides

In this section, we discuss the grain-size distributions and composition of FeTi oxides that originally crystallize from igneous melts. These original phases are referred to as *primary FeTi oxides*.

Both titanomagnetites and titanohematites crystallize at $\sim 1300^\circ\text{C}$ and are early in the crystallization sequences of igneous rocks. Cooling rate has a major effect on grain-size distribution of FeTi oxides. Rapidly cooled volcanic rocks (such as oceanic pillow basalts) often contain titanomagnetites with a significant proportion of grains in the $1\text{-}\mu\text{m}$ or smaller sizes. These fine-grained titanomagnetites often display delicate skeletal crystalline habits. Slowly cooled intrusive rocks usually contain larger grain sizes, sometimes exceeding $100\ \mu\text{m}$. As we shall discover later, fine-grained ferromagnetic particles are the best magnetic recorders. This is one of the reasons why volcanic rocks are preferred over intrusive rocks as targets for paleomagnetic study.

As a result of magmatic differentiation processes, mafic igneous rocks tend to have a higher fraction of primary FeTi oxides (and those oxides contain higher Ti:Fe ratio) than do felsic igneous rocks. In basalts, both titanomagnetite and titanohematite are primary FeTi oxides. Compositions of primary titanomagnetites are usually within the range $0 < x < 0.8$, while primary titanohematite is almost pure ilmenite with $0.8 < x < 0.95$. Primary titanohematite is thus paramagnetic under ambient surface conditions. Total FeTi oxide content of basalts is typically 5% by volume, with approximately equal parts titanomagnetite and titanohematite.

Silicic igneous melts have higher oxygen fugacity, f_{O_2} , than mafic melts. Felsic rocks have lower content of FeTi oxides, and those FeTi oxides have lower Ti content. Primary titanomagnetites are Ti-poor approaching magnetite, and titanohematites are hematite rich. Although primary titanomagnetites of intermediate composition are common, intermediate composition titanohematites in the $0.4 < x < 0.8$ range are relatively rare. Most primary titanohematites in mafic and intermediate igneous rocks are Ti-rich, with occasional Ti-poor titanohematites in silicic rocks.

In addition to primary FeTi oxides that crystallize from igneous melts, Ti-poor titanomagnetite is often exsolved from plagioclase or pyroxene in plutonic rocks (Figure 2.11a). Although a small fraction of the total

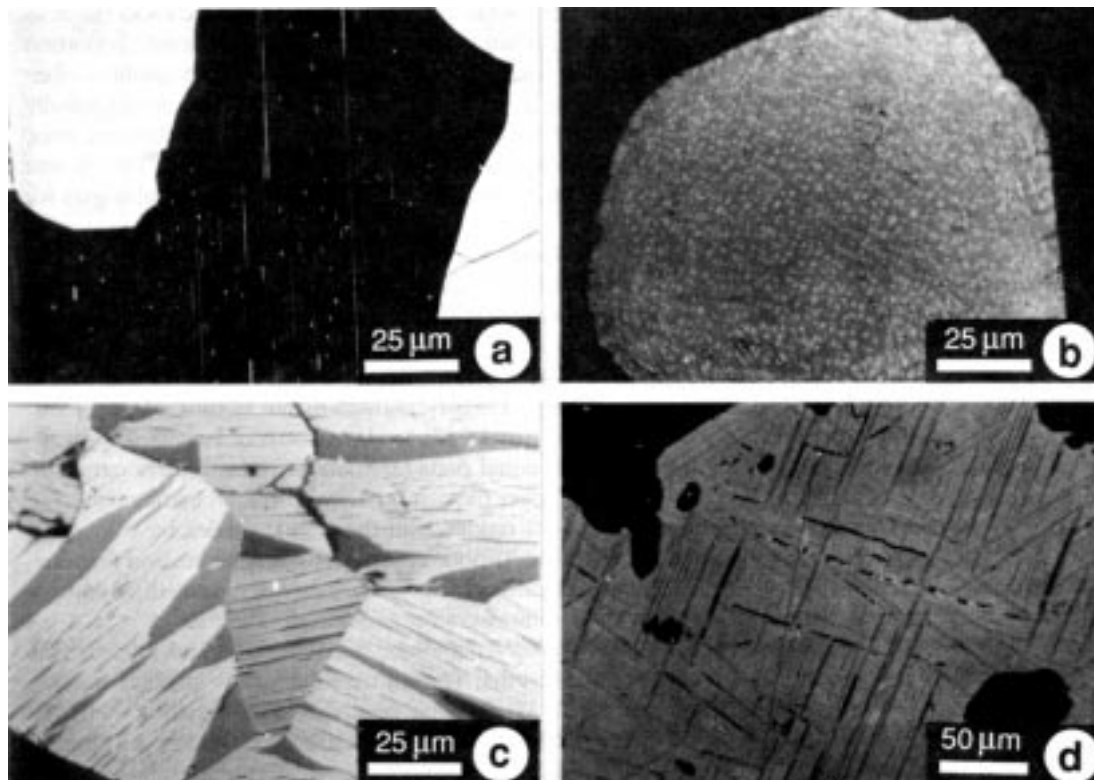


Figure 2.11 Micrographs of FeTi-oxide minerals. (a) Optical photomicrograph of exsolved rod-shaped grains of titanomagnetite (small white grains) within a plagioclase crystal. (b) Optical photomicrograph of exsolution of magnetite grains (white) within ulvöspinel (gray). (c) Optical photomicrograph of Ti-rich titanohematite (dark-gray lenses) within light-gray host Fe-rich titanohematite. (d) Optical photomicrograph of ilmenite lamellae within titanomagnetite grain; note the symmetry of the ilmenite planes that are parallel to (111) planes of the host titanomagnetite. Photomicrographs kindly provided by S. Haggerty.

FeTi oxides, these titanomagnetites are fine-grained and can be effective paleomagnetic recorders. During original cooling of igneous rocks, primary FeTi oxides can be affected by solid state exsolution and/or deuteric oxidation. Both processes can alter compositions and grain size of FeTi oxides, with profound effects on magnetic properties.

Exsolution

Both titanomagnetites and titanohematites crystallize at $\sim 1300^{\circ}\text{C}$, and solid solution is complete at these high temperatures. Thus, all compositions are possible at high temperature. However, at lower temperatures, compositional gaps develop below the curves shown in Figure 2.12. At temperatures below these curves, intermediate compositions unmix or *exsolve* into Ti-rich regions and Ti-poor regions by solid state diffusion of Fe and Ti cations. However, diffusion is sluggish at low temperatures, so rapid cooling can preserve intermediate compositions. Because titanomagnetites unmix at fairly low temperature ($\sim 600^{\circ}\text{C}$), exsolution is slow and is generally observed only in slowly cooled plutonic rocks. Compositional gaps develop at higher temperatures in the titanohematite series, and exsolution is more rapid.

Exsolution of intermediate composition titanomagnetites and titanohematites is important for two reasons:

1. Unmixing of intermediate-composition grains into composite grains with Ti-rich and Ti-poor regions alters magnetic properties such as j_s and T_C that depend on composition.
2. Exsolution dramatically decreases effective grain size.

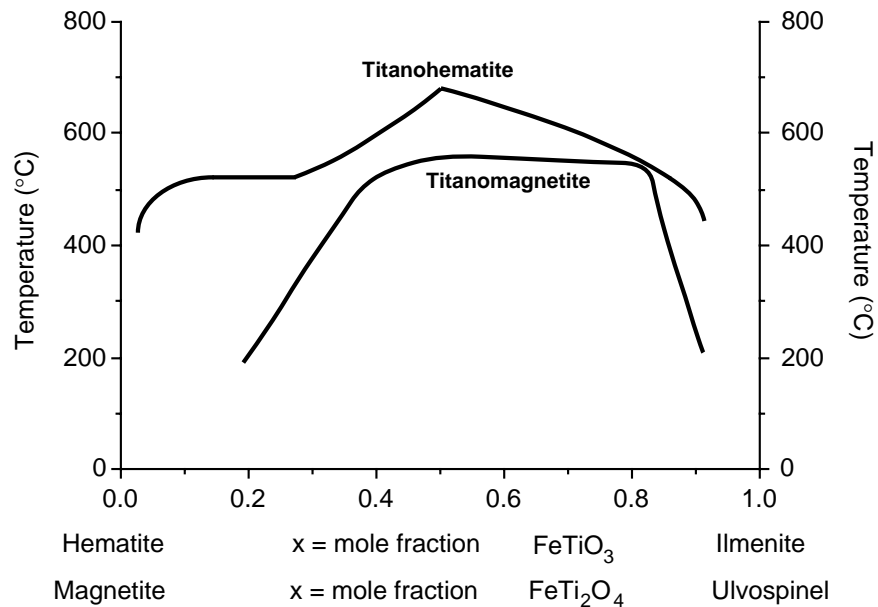


Figure 2.12 Compositional gaps for titanohematite and titanomagnetite. Compositions are indicated by parameter x for each series; solid solution is complete within each series at temperatures above the bold curves; exsolution occurs for intermediate compositions at temperatures below these curves. Adapted from Nagata (1961) and Burton (*Reviews in Mineralogy*, v. 24, in press).

By exsolution, a large homogeneous grain is transformed into a composite grain of much smaller Ti-poor (Fe-rich) regions and complementary Ti-rich (Fe-poor) regions. In titanomagnetite, exsolution yields Ti-poor crystals of cubic habit surrounded by Ti-rich regions (Figure 2.11b). The resulting composite grain will have fine-grained crystals of ferromagnetic, Ti-poor titanomagnetite surrounded by paramagnetic, Ti-rich titanomagnetite. A similar situation occurs for exsolved titanohematite, except that exsolution occurs along (0001) planes, yielding a *tiger-striped* composite grain (Figure 2.11c). As will be discussed in the following chapter, the decrease in grain size of ferromagnetic particles that accompanies exsolution has a profound influence on magnetic properties.

Deuteric oxidation

Oxidation that occurs during original cooling of an igneous rock is *deuteric oxidation*. During cooling, the primary FeTi-oxide grains are often out of equilibrium with the temperature and oxygen conditions. Deuteric oxidation almost always occurs unless the rock is rapidly cooled and/or under pressure (e.g., seafloor conditions) where degassing does not occur.

Extensive studies of deuteric oxidation in basalts indicate that typical conditions of deuteric oxidation involve temperatures of 750°C and $f\text{O}_2$ of 10^{-5} – 10^{-6} atmospheres. Deuteric oxidation occurs in the solid state but generally above the Curie temperature. Both primary titanomagnetite and primary titanohematite are affected by deuteric oxidation. As an example, consider the commonly observed effects of deuteric oxidation on primary titanomagnetite in a basalt. The path of compositional change due to oxidation is shown in Figure 2.13. Composition of primary titanomagnetite is $x = 0.6$, typical of basalts. Oxidation generally takes place along paths of constant Ti:Fe ratio parallel to the base of the ternary diagram. The $\text{Fe}^{3+}:\text{Fe}^{2+}$ ratio increases during oxidation, driving composition toward the right. However, the resulting grain is not usually homogeneous, but rather is a composite grain with ilmenite lathes along (111) planes of the host titanomagnetite (Figure 2.11d). The composition of host titanomagnetite becomes enriched in Fe and approaches pure magnetite.

The compositional change of the titanomagnetite resulting from deuteric oxidation changes the magnetic properties. An Fe-rich titanomagnetite with both higher Curie temperature and higher saturation mag-

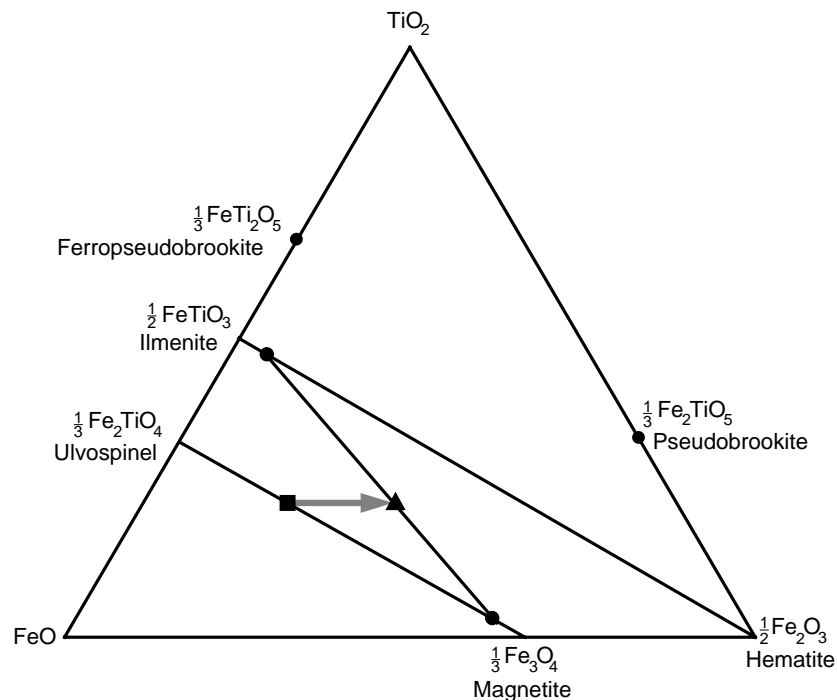


Figure 2.13 TiO_2 – FeO – Fe_2O_3 ternary diagram. Composition of primary $x = 0.6$ titanomagnetite is shown by the square; the stippled arrow shows the change in composition during deuteritic oxidation; the circles connected by solid lines show the mineral compositions resulting from deuteritic oxidation.

netization replaces primary titanomagnetite of intermediate composition. In addition, grain size is drastically decreased, the primary grain now being subdivided into many smaller grains separated by paramagnetic ilmenite. Again, this decreased grain size has a major effect on magnetic properties.

There are stages of deuteritic oxidation, and the stage to which the FeTi oxides of a particular igneous rock evolve depends on cooling rate and $f\text{O}_2$. Primary Ti-rich titanohematite also undergoes deuteritic oxidation; extreme cases yield grains that are composites of *rutile* (TiO_2), hematite ($\alpha\text{Fe}_2\text{O}_3$), and sometimes *pseudobrookite* (Fe_2TiO_5). Similarly, extreme deuteritic oxidation of primary titanomagnetite can yield rutile plus hematite. Dramatic examples of the importance of deuteritic oxidation to magnetic properties have been provided by examination of FeTi oxides and magnetic properties of samples collected from profiles through single basalt flows. Intensity and stability of paleomagnetism are commonly maximized in interior zones where deuteritic oxidation proceeded to advanced stages.

Low-temperature oxidation

Weathering of titanomagnetites at ambient surface temperatures, or hydrothermal alteration at $T < 200^\circ\text{C}$, can lead to the production of *cation deficient spinels*. The classic example is oxidation of magnetite to yield *maghemite* ($\gamma\text{Fe}_2\text{O}_3$), which is chemically equivalent to hematite ($\alpha\text{Fe}_2\text{O}_3$) but retains the spinel crystal structure.

In studying the low-temperature oxidation process, it is instructive to use a *structural formula* with brackets indicating cations in the B sublattice. For instance, magnetite can be written $\text{Fe}^{3+}[\text{Fe}^{3+}\text{Fe}^{2+}]_2\text{O}_4$, indicating that each formula unit of magnetite has one Fe^{3+} in the A sublattice and one Fe^{3+} plus one Fe^{2+} in the B sublattice. The structural formula for maghemite is $\text{Fe}^{3+}[\text{Fe}^{3+}\text{Fe}^{3+}_{2/3}\square_{1/3}]_2\text{O}_4$, indicating that magnetite is oxidized to maghemite by changing the valence state of two thirds of the original Fe^{2+} to Fe^{3+} while simultaneously removing one third of the original Fe^{2+} from the B sublattice. This removal occurs by diffusion producing *vacancies* (\square) in the spinel structure where a Fe^{2+} cation had previously resided; these vacan-

cies account for the name cation-deficient spinel. Because ferrimagnetism of magnetite results from Fe^{2+} in the B sublattice, removal of one third of these cations decreases saturation magnetization from 480 G (4.8×10^5 A/m) for magnetite to 420 G (4.2×10^5 A/m) for maghemite. Maghemite is usually metastable and irreversibly changes crystal structure to hexagonal $\alpha\text{Fe}_2\text{O}_3$ on heating to $300^\circ\text{--}500^\circ\text{C}$.

Similar low-temperature oxidation of titanomagnetites produces cation-deficient titanomaghemites. Titanomagnetite (composition $x = 0.6$) is the dominant primary FeTi oxide in oceanic pillow basalts, which comprise the upper 0.5 km of oceanic crust. During seafloor weathering, titanomagnetites oxidize to titanomaghemite with attendant decrease in intensity of magnetization, producing a major decrease in amplitude of resulting marine magnetic anomalies. Consequently, titanomaghemite is one of the most abundant FeTi oxides in the earth's crust.

It has been recognized recently that formation of maghemite is primarily responsible for increased ferromagnetic mineral content in soils. Besides the oxidation of detrital magnetite, three processes are responsible:

1. Formation of maghemite (and sometimes magnetite) from iron oxides or oxyhydroxides by repeated oxidation-reduction cycles during soil formation;
2. Natural burning in the presence of organic matter; temperatures above $\sim 200^\circ\text{C}$ aid in conversion of paramagnetic Fe-bearing minerals to maghemite;
3. Dehydration of lepidocrocite (γFeOOH), a common iron-oxyhydroxide weathering product of iron silicates.

Iron oxyhydroxides and sulfides

Oxyhydroxides of iron are common in weathered igneous and metamorphic rocks, in soils, and in sediments. The most important oxyhydroxide is goethite (αFeOOH), which is the stable form of iron oxide in soils of humid regions and also results from alteration of pyrite (FeS_2) in limestones. Goethite is orthorhombic and antiferromagnetic with a Néel temperature of 120°C , but natural goethite commonly displays weak ferromagnetism. Natural dehydration of goethite (or laboratory heating to $300^\circ\text{--}400^\circ\text{C}$) produces hematite and is an important process in formation of red sediments. Lepidocrocite (γFeOOH) is an oxyhydroxide with cubic crystal structure and is paramagnetic at room temperature (Néel temperature of -196°C). Lepidocrocite often converts to goethite or to maghemite by dehydration.

Formation of iron sulfides is a crucial concern in regard to paleomagnetic records in marine sediments, and we will return to this subject in Chapter 8. At this point, we just develop the basic magnetic properties of these minerals. Iron sulfides can occur naturally with compositions ranging from pyrite (FeS_2) to troilite (FeS), although the latter is common only in meteorites. A general chemical formula can be written FeS_{1+x} ($0 \leq x \leq 1$) and compositions of iron sulfides can be expressed by the compositional parameter x . Pyrrhotite is a ferrimagnetic iron sulfide with monoclinic crystal structure with composition in the Fe_7S_8 to Fe_9S_{10} range ($0.11 \leq x \leq 0.14$). Two antiparallel coupled sublattices containing Fe cations are present, but inequalities develop in the number of Fe cations in opposing sublattices. Thus, pyrrhotite is ferrimagnetic. The Curie temperature is 320°C , and saturation magnetization can reach 130 G (1.3×10^5 A/m). Pyrrhotite generally forms during diagenesis of marine sediments in depositional environments with abundant organic input but can also form in metamorphic aureoles surrounding igneous intrusives.

SUGGESTED READINGS

- S. Chikazumi, *Physics of Magnetism*, Wiley, New York, 554 pp., 1964.
An excellent introduction to physics of magnetism.
- D. H. Lindsley, The crystal chemistry and structure of oxide minerals as exemplified by the Fe-Ti oxides, in: *Oxide Minerals*, ed: D. Rumble, III, Mineralogical Society of America, Washington, D.C., 1976a, pp. L1–L60.
- D. H. Lindsley, Experimental studies of oxide minerals, in: *Oxide Minerals*, ed: D. Rumble, III, Mineralogical Society of America, Washington, D.C., 1976b, pp. L61–L88.

These two articles present in-depth discussion of mineralogy of Fe-Ti oxides and experimental data pertaining to exsolution.

S. E. Haggerty, Oxidation of opaque minerals in basalts, in: *Oxide Minerals*, ed: D. Rumble, III, Mineralogical Society of America, Washington, D.C., 1976a, pp. Hg1–Hg100.

S. E. Haggerty, Opaque mineral oxides in terrestrial igneous rocks, in: *Oxide Minerals*, ed: D. Rumble, III, Mineralogical Society of America, Washington, D.C., 1976b, pp. Hg101–Hg300.

These two articles present detailed observations of deuteric oxidation; they include many insightful polished section photomicrographs.

T. Nagata, *Rock Magnetism*, Maruzen Ltd., Tokyo, 350 pp., 1961.

Chapters 1–3 provide a thorough (although sometimes outdated) introduction to magnetic properties of ferromagnetic minerals.

F. D. Stacey and S. K. Banerjee, *The Physical Principles of Rock Magnetism*, Elsevier, Amsterdam, 195 pp., 1974.

Chapters 1 and 2 concern magnetic properties of solids and magnetic minerals.

R. Thompson and F. Oldfield, *Environmental Magnetism*, Allen and Unwin, London, 227 pp., 1986.

Chapters 2 through 4 discuss magnetic properties of solids and magnetic minerals.

PROBLEMS

- 2.1** Fayalite (Fe_2SiO_4) is a paramagnetic solid with magnetic susceptibility $\chi = 4.4 \times 10^{-4}$ emu at 0°C ($= 273^\circ\text{K}$).
- A single crystal of fayalite has volume $= 2 \text{ cm}^3$. This crystal is placed in a magnetic field, $H = 10$ Oe, at 0°C . What is the resulting magnetic dipole moment, M , of this crystal?
 - If fayalite is placed in a magnetic field, $H = 100$ Oe, at a temperature of 500°C ($= 773^\circ\text{K}$), what is the resulting magnetization, J ?
- 2.2** MnS is a paramagnetic solid. At 300°K , there are 4×10^{22} molecules of MnS per cm^3 . If the cationic magnetic moment of Mn^{2+} is $5 M_B$, what is the paramagnetic susceptibility, χ , of MnS at 300°K ?